

# RSC Advances



This is an *Accepted Manuscript*, which has been through the Royal Society of Chemistry peer review process and has been accepted for publication.

*Accepted Manuscripts* are published online shortly after acceptance, before technical editing, formatting and proof reading. Using this free service, authors can make their results available to the community, in citable form, before we publish the edited article. This *Accepted Manuscript* will be replaced by the edited, formatted and paginated article as soon as this is available.

You can find more information about *Accepted Manuscripts* in the [Information for Authors](#).

Please note that technical editing may introduce minor changes to the text and/or graphics, which may alter content. The journal's standard [Terms & Conditions](#) and the [Ethical guidelines](#) still apply. In no event shall the Royal Society of Chemistry be held responsible for any errors or omissions in this *Accepted Manuscript* or any consequences arising from the use of any information it contains.

# SYNTHESIS AND ELECTROCHEMICAL BEHAVIOUR OF NiFeCr NANOPARTICLE COATING

Rohit Berlia\*, Punith Kumar MK\* and Chandan Srivastava\*#

\*Department of Materials Engineering, Indian Institute of Science, Bangalore-560012, India

\*Corresponding author. Tel: +91-80-22932834

E-mail address: csrivastava@materials.iisc.ernet.in (Chandan Srivastava)

## Abstract

NiFeCr nanoparticles with Ni-rich composition were synthesized using the wet chemical synthesis technique. As synthesized nanoparticles were crystalline with an average size of  $6.8 \pm 2.5$  nm. For electrochemical analysis, as-synthesized nanoparticles were mixed with epoxy and coated over a mild steel substrate. Electrochemical measurements exhibited a very high polarization resistance and very low corrosion current for the nanoparticle-epoxy coated sample illustrating high resistance of NiFeCr nanoparticle-epoxy coating towards highly corrosive media.

**Keywords:** Ni-Fe-Cr nanoparticles, Corrosion, Coating, Superalloy, Inconel.

## Introduction

Family of nickel based superalloys containing Cr and Fe, commonly known as inconel, have been explored extensively because of their remarkable high temperature strength and resistance to degradation in highly corrosive and oxidizing environments.<sup>1-4</sup> These alloys are now standard engineering material with extensive usage in rocket engines, power-generation turbines, chemical processing environments, nuclear plants etc. Superalloys are generally manufactured as bulk solids, foils and micron size powders. There are extremely few reports in the literature on synthesis and properties of superalloys in isolated ultra-fine geometries such as nanowires and nano-particles.<sup>5</sup> Investigation of properties of superalloys in isolated nano-scale geometries or in

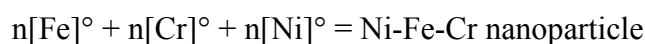
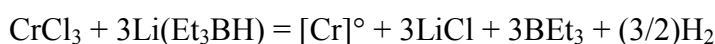
geometries made from consolidating individual nanosolids can be scientifically interesting and technologically relevant as these investigations may reveal some completely novel properties emerging from the synergy between extremely high specific surface area, elemental composition and size dependent microstructure. Dispersions of crystalline superalloy nanoparticles can provide important advantages such as (a) they can be conveniently sprayed over an engineered surface, (b) they can form ultra-thin protective films and thus facilitate weight reduction, (c) annealing of thin nanoparticle coatings can cause particle-to-particle sintering which can facilitate gradual tuning of the grain size dependent attributes such as mechanical properties<sup>6,7</sup>, corrosion resistance<sup>8</sup> etc, (d) superalloy nanoparticles can be mixed with Ag nanoparticles to provide ultra thin coatings with anti-microbial properties<sup>9</sup>, (e) foreign materials such as graphene can be mixed in superalloy nanoparticle dispersion to produce coating with tunable electrical and thermal conductivities<sup>10,11</sup> etc.

Present work provides a wet chemical synthesis route to produce sub 10 nm sized crystalline Ni rich, Ni-Fe-Cr nanoparticles. Chemical synthesis technique is a convenient method for producing large quantities of single and multi-component nanoparticles.<sup>12</sup> It is shown that as-synthesized NiFeCr nanoparticles exhibit very high corrosion resistance properties.

## Experiment

To synthesize Ni-Cr-Fe nanoparticles, 0.3 g of NiCl<sub>2</sub>.6H<sub>2</sub>O, 0.034 g of FeCl<sub>2</sub>.4H<sub>2</sub>O and 0.0691 g of CrCl<sub>3</sub>.6H<sub>2</sub>O were dissolved in 25 mL of diphenyl ether solvent contained in a three neck round bottom flask fitted with a reflux condenser and a magnetic stirrer. Nanoparticle synthesis reaction occurred under an argon atmosphere. The reaction mixture was heated to 110°C and at this temperature, 0.2 mL of oleic acid and 0.2 mL of oleylamine were added into the reaction mixture using a syringe. Temperature of the reaction mixture was then increased to

200°C. At this temperature, 7 mL of superhydride (LiBEt<sub>3</sub>H) was injected slowly into the reaction mixture. Temperature of the reaction mixture was then raised to the boiling temperature of the reaction mixture and refluxed for one hour. After one hour, the reaction mixture was cooled to the room temperature. At room temperature, ethanol was added into the reaction mixture to sediment the nanoparticles which were subsequently isolated by centrifugation. Chemical reactions during the formation of alloy nanoparticles are:



To prepare the epoxy-nanoparticle composite coating, 50 mg of nanoparticle was mixed with 0.68 g of epoxy (EPOLAM 8025). This mixture was then heated at 50° C for 30 minutes to enhance the fluidity of the epoxy in order to uniformly disperse the nanoparticles into it. Thereafter, hardener (amine hardener) was added into the epoxy-nanoparticle mixture. This mixture was maintained at 50°C for ~10 min. Weight ratio of epoxy-to-hardener was 100:38. The nanoparticle-epoxy-hardener mixture was then drop-dried over mild steel substrate. The coating was then allowed to cure for 24 hours at the room temperature.

Average composition of the nanoparticle dispersion was determined by energy dispersive spectroscopy (EDS) technique using a Quanta ESEM scanning electron microscope (SEM) operating at 20 kV. SEM was also used to inspect the nanoparticle coating before and after the electrochemical analysis. X-ray diffraction (XRD) profile from as-synthesized nanoparticles was obtained using X-pert pro X-ray diffractometer employing a Cu K<sub>α</sub> radiation ( $\lambda = 0.1540$  nm) source. A 300 keV field emission FEI Tecnai F-30 transmission electron microscope (TEM) was

used to obtain TEM bright field images, selected area electron diffraction (SAD) patterns and compositional information using the scanning transmission electron microscopy–EDS (STEM-EDS) technique. A highly dilute dispersion of as-synthesized nanoparticles was drop dried onto a carbon coated Cu grid for the TEM based analysis. Electrochemical corrosion behavior of the samples was analyzed by CHI electrochemical workstation (US make) with conventional three electrode cell and 3.5% NaCl solution as an electroactive media. Pt foil and Ag/AgCl electrode was used as counter and reference electrode respectively. In three separate experiments, bare mild steel coupons, only epoxy coated mild steel coupons and nanoparticle mixed with epoxy coated mild steel coupons of 1 cm<sup>2</sup> area were used as working electrode.

## Result and Discussion

A representative low magnification TEM bright field image of as-synthesized nanoparticles is shown in Fig. 1(a). It can be observed that the synthesis procedure has produced nearly spherical nanoparticles. Average size calculated from the summation average of sizes of ~200 individual nanoparticles was 6.8±2.5 nm. Average composition of nanoparticles obtained from the SEM-EDS analysis was 78% at% Ni, 12 at% Cr and 10 at% Fe. SAD pattern obtained from the nanoparticles in TEM is shown as insert in Fig 1(a). Presence of circular rings in the SAD pattern indicates that the as-synthesized nanoparticles were crystalline in nature. Analysis of particle crystallinity at a single nanoparticle level using high resolution TEM (HRTEM) revealed that the nanoparticles were both single and polycrystalline. A qualitative analysis indicated that the relative percentage of nanoparticles with polycrystalline microstructure was greater than the single crystalline nanoparticles. Representative HRTEM image of smaller nanoparticles, nanoparticles with single crystalline microstructure and a polycrystalline large sized nanoparticle is shown respectively in Fig. 1(b), 1(c) and 1(d). Changes in the direction of

the lattice fringes indicate polycrystallinity. STEM-EDS compositional analysis of several individual nanoparticles revealed the presence of all the three components (Ni, Fe, Cr) within the nanoparticles. A representative STEM-EDS compositional profile revealing peaks corresponding to Ni, Fe and Cr elements is shown in Fig. 1(e). Insert in Fig. 1(e) shows the STEM-HAADF (high angle annular dark field) image of the nanoparticle (encircled) from which the EDS data was collected. The electron probe size used in the STEM-EDS analysis was  $\sim 2$  nm. XRD profile obtained from as-synthesized nanoparticles is shown in Fig. 1(f). Major peaks in the XRD profile correspond to Ni-rich phase. It should be noted that the peaks labeled 'Ni' in Fig. 1(f) are shifted with respect to the pure Ni phase peak indicating alloying of Ni with Fe and Cr atoms. Other minor peaks in the XRD profile were identified to correspond to Ni-O, Cr-O and Ni-Cr phases. These minor phase volumes may be present independently as nanoparticles or as one of the phases in polycrystalline nanoparticles. Nanoparticle average size calculated from the full width at half maximum (FWHM) of the (111) Ni peak and the Scherrer formula<sup>13</sup> was found to be 5 nm. Average size values calculated from the Scherrer formula is less than the average size value calculated from measuring sizes of individual nanoparticles. This observation indicates that the number of polycrystalline nanoparticles in the dispersion is greater than the number of single crystalline nanoparticles.

A representative high magnification SEM micrograph of only epoxy coating is shown in Fig. 2(a). It can be seen in Fig. 2(a) that the epoxy coating is smooth and does not contain micro-cracks and pinholes. Compositional line scans conducted using the SEM-EDS technique did not reveal any Fe content. EDS signal corresponding to Fe can appear from the underlying steel substrate if micro-cracks or pinholes are present. SEM micrographs and compositional analysis

therefore strongly indicated towards a negligible presence of microcracks and pinholes in the epoxy film.

SEM micrograph of as-deposited nanoparticle-epoxy coating is shown in Fig. 2(b). It can be seen that the as-deposited coating is macroscopically smooth. To determine the uniformity of nanoparticle dispersion in the epoxy coating, SEM-EDS compositional mapping experiment was conducted. A representative compositional mapping result is provided in Fig. 2(c). A fairly uniform distribution of Ni, Fe and Cr atoms in the region of interest in Fig. 2(c) illustrates a uniform distribution of nanoparticles in the epoxy coating. A minor degree of nanoparticle agglomeration represented by the brighter spots in Fig. 2(c) was also observed. Thickness of the coating determined from the cross-section SEM image was  $\sim 121 \mu\text{m}$ . Cross section SEM micrograph showing coating thickness over steel substrate is provided in Fig. 2(d).

SEM micrographs of bare mild steel substrate, epoxy coating and nanoparticle-epoxy coating after electrochemical test showing the formation of corrosion product is provided respectively in Fig. 3(a-c). Corrosion products that could have formed from NiFeCr nanoparticle are oxides and hydroxides of component metals.<sup>14,15,16</sup> Corrosion products that could have formed from epoxy are alcohols and aldehydes.<sup>17</sup>

Potentiodynamic polarization study was conducted in order to quantify the kinetic parameters of the corrosion process. Tafel polarization curves were obtained by varying the applied potential by  $\pm 200 \text{ mV}$  from the open circuit potential (OCP) value at the scan rate of  $10 \text{ mV s}^{-1}$ . The recorded Tafel plots are shown in Fig 4(a). As seen in the Fig 4(a), corrosion potential ( $E_{\text{corr}}$ ) of only epoxy coated and nanoparticles-epoxy coated samples are shifted towards less negative potential when compared to the  $E_{\text{corr}}$  of uncoated mild steel substrate.  $E_{\text{corr}}$  values for bare mild steel substrate, epoxy coated and nanoparticles-epoxy coated samples were

0.618V, -0.470V and -0.452V respectively. These values reveal that between the three samples, nanoparticle-epoxy coated sample was most corrosion resistant. Corrosion current ( $I_{\text{corr}}$ ) value for bare mild steel substrate, only epoxy coated and nanoparticles-epoxy coated samples were found to be  $15.65 \mu\text{Acm}^{-2}$ ,  $2.311 \mu\text{Acm}^{-2}$  and  $1.085 \mu\text{Acm}^{-2}$  respectively. Corrosion current which is direct indication of the corrosion rate is drastically reduced after coating of only epoxy resin over the mild steel substrate. Addition of Ni-Fe-Cr nanoparticles into the epoxy resin coating facilitated further reduction in the corrosion current and increment in the corrosion potential. The electrochemical impedance data was measured at the OCP value in the 100 mHz - 1 MHz frequency range at the data density of 6 points per decade frequency with sinusoidal signal amplitude of 5 mV. The measured EIS data is presented as typical Nyquist plot in Fig 4(b). Two capacitive loops in the Nyquist plot in Fig. 4(b) indicate that the corrosion process involved two relaxation events for all the three samples. As seen in Fig 4(b), width of the capacitive loop, which is a measure of the corrosion resistance or polarization resistance ( $R_p$ ), however, varied between the three samples considerably. Using the electrical equivalent circuit shown in Fig 4(c), polarization resistance value for the mild steel substrate, epoxy coated and nanoparticle-epoxy coated substrate was calculated to be 771  $\Omega$ , 12700  $\Omega$  and 30100  $\Omega$  respectively. It can be observed that nanoparticle-epoxy coating increased the polarization resistance considerably.

## Conclusion

Wet chemical synthesis method was used to produce Ni-Fe-Cr nanoparticles. As synthesized nanoparticles were crystalline with sub-10 nm dimensions. Electrochemical analysis of coating of nanoparticles-mixed-in-epoxy over steel substrate revealed high corrosion potential, low

corrosion rate and high polarization resistance. This clearly indicated that the nanoparticle-epoxy composite coating is highly resistive towards aggressive corrosive environments.

### **Acknowledgement**

Authors acknowledge the electron microscopy facilities at the Advanced Facility for Microscopy and Microanalysis (AFMM) IISc, Bangalore. Authors also acknowledge the funding received from the SERB, Govt of India and JATP, Indian Institute of Science. Prof. Suryasarathi Bose, Materials Engineering, IISc is thanked for providing the epoxy used in the investigation.

## References

- 1 T. M. Pollock and S. Tin, *J.Propul.Power.*, 2006, **22**(2), 361.
- 2 G. P. Sabol and R. Stickler, *Phys. Stat. Sol.*, 1969, **35**, 11.
- 3 ShMukhtarov and A Ermachenko, *Journal of Physics: conference series*, 2010, **240**(1), 012118.
- 4 M. Liu, J. Zheng, Y. Lu, Z. Li, Y. Zou, X. Yu and X. Zhou, *J. Nucl. Mater.*, 2013, **440**, 124.
- 5 R. Berlia, M. P. Singh, P. Kumar MK, and C. Srivastava, *ECS Electrochem. Lett.*, 2015, **4**(2), D1.
- 6 J. R. Greer and R. A. Street, *J. Appl. Phys.*, 2007, **101**, 103529.
7. N. Wang, Z. Wang, K.T. Aust, U. Erb, *Acta Mater.*, 1995, **43**(2), 519.
8. K. D. Ralston and N. Birbilis, *Corrosion*, 2010, 66(7), 075005.
9. J. S. Kim, E. Kuk, K. N. Yu, J. H. Kim, S. J. Park, H. J. Lee, S. H. Kim, Y. K. Park, Y. H. Park, C. Y. Hwang, Y. K. Kim, Y. S. Lee, D. H. Jeong and M. H. Cho, *Nanomed-Nanotechnol.* 2007, **3**(1), 95.
10. S. Stankovich, D. A. Dikin, G. H. B. Dommett, K. M. Kohlhaas, E. J. Zimney, E. A. Stach, R. D. Piner, S. T. Nguyen and R. S. Ruoff, *Nature*, 2006, **442**, 282.
11. Q. Li, Y. Guo, W. Li, S. Qiu, C. Zhu, X. Wei, M. Chen, C. Liu, S. Liao, Y. Gong, A. K. Mishra and L. Liu, *Chem. Mater.*, 2014, **26**, 4459.
12. B. H. Kim, M. J. Hackett, J. Park, and T. Hyeon, *Chem. Mater.*, 2014, **26**(1), 59.
13. A. Patterson, *Phys. Rev.*, 1939, **56**(10), 978.
14. S. V. Yadla, V. Sridevi, M.V.V.C. Lakshmi, S.P.K. Kumari, *International Journal of Engineering Science and Advanced Technology*, 2012, **2**(3), 637.
15. R. E. Hummel, R. J. Smith and E. D. Verink JR, *Corros. Sci.*, 1987, **27**(8), 803.

16. B. Zhang, J. Wu, X. Li, H. Liu, B. Yadian, R. V. Ramanujan, K. Zhou, R. Wu, S. Hao, and Y. Huang, *J. Phys. Chem. C*, 2014, **118**, 9073.
17. N. Grassie and M. I. Guy, *Polym. Degrad. Stabil.*, 1985, **13**, 11.

### Figure Captions

**Fig.1(a)** TEM bright field image of as-synthesized Ni-Fe-Cr nanoparticles, **(b)** HRTEM image of smaller nanoparticles, **(c)** HRTEM images of single crystalline nanoparticles, **(d)** HRTEM images of a large sized polycrystalline nanoparticle, **(e)** STEM-EDS curve obtained from a single nanoparticle. Insert in Fig. 1(e) shows the STEM-HAADF image of the nanoparticle (circled) from which the EDS data was obtained, **(f)** XRD profile obtained from as-synthesized nanoparticles. Information about crystal plane direction, interplanar distance and miller index is also provided in Fig 1(c) and Fig. 1(d). Carbon, copper and chlorine peaks in the EDS spectrum are from the carbon coated Cu grid used to hold the samples. Oxygen peak is due to the surfactant surrounding the nanoparticles.

**Fig. 2(a)** SEM micrograph of only epoxy coating, **(b)** SEM micrograph of nanoparticle-epoxy coating, **(c)** EDS compositional mapping results showing the distribution of Ni, Fe, and Cr elements in a region of interest. **(d)** SEM micrograph showing the coating thickness

**Fig. 3** Representative SEM micrograph of **(a)** steel substrate, **(b)** epoxy coating and **(c)** nanoparticle-epoxy coating after corrosion experiment.

**Fig. 4(a)** Potentiodynamic polarization curves for mild steel, epoxy coated mild steel and nanoparticles-epoxy coated mild steel recorded in 3.5% NaCl media against Ag/AgCl reference electrode, **(b)** Impedance Nyquist plots corresponding to mild steel, epoxy coated mild steel and nanoparticles-epoxy coated mild steel recorded in 3.5% NaCl media against Ag/AgCl reference electrode. Inset shows the Nyquist plot for mild steel substrate and **(c)** electrical equivalent circuit used to calculate the polarization resistance from impedance Nyquist curves.

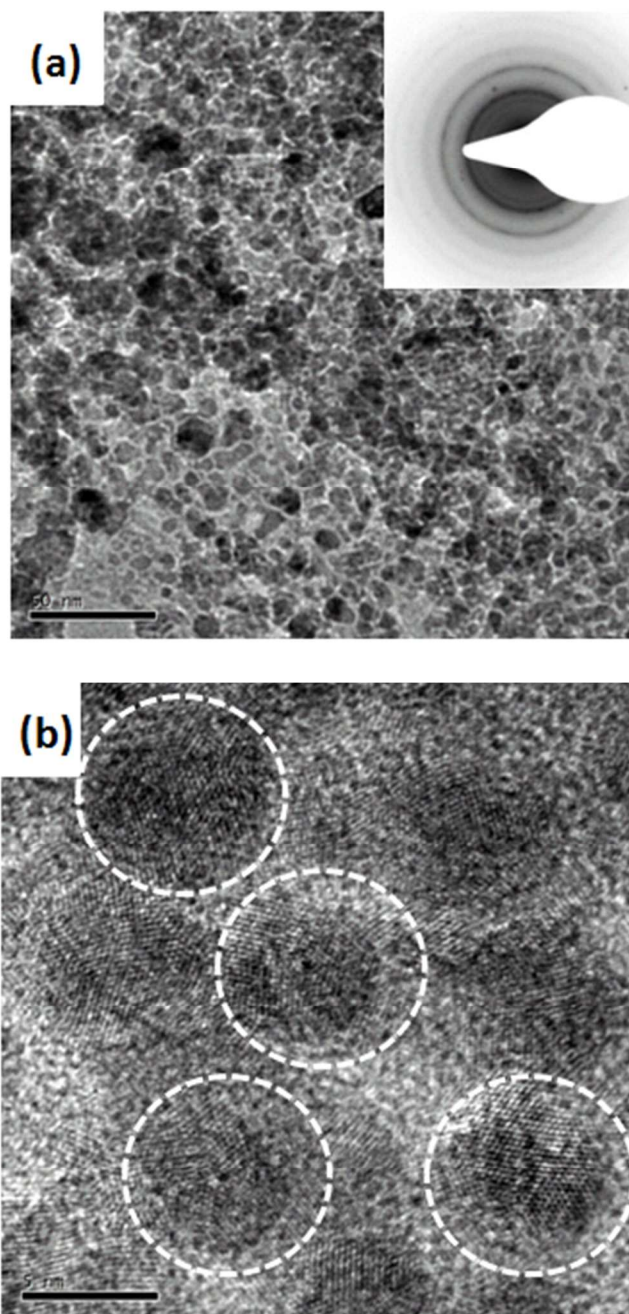


**Figure 1**

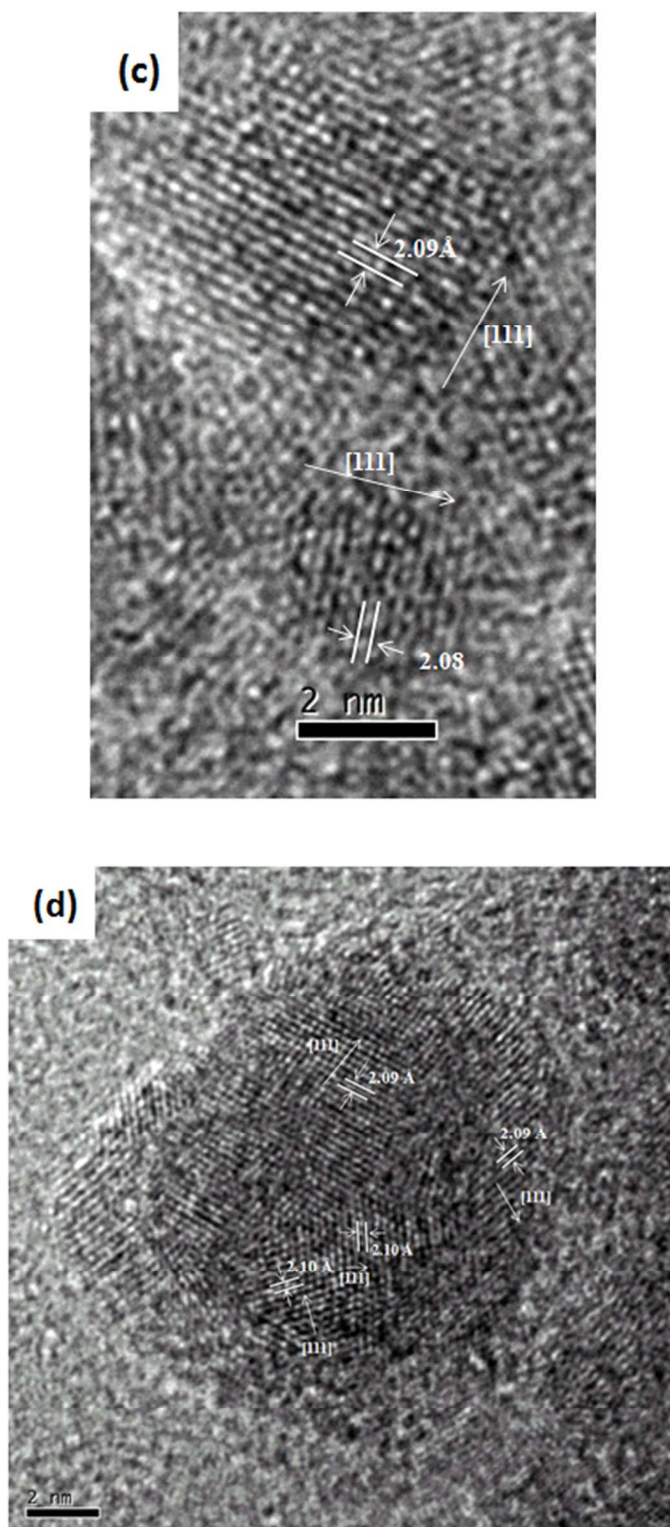


Figure 1

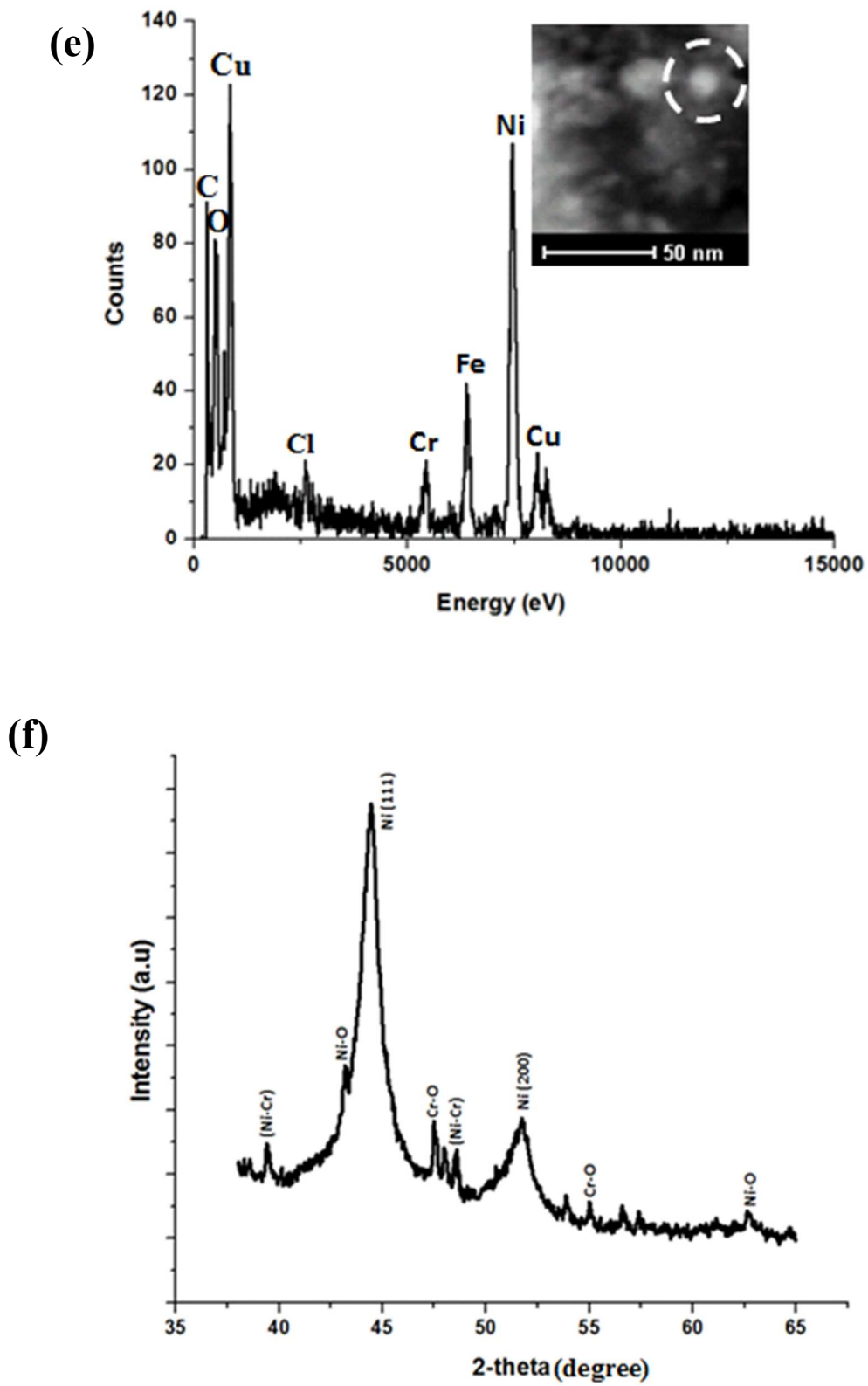


Figure 1

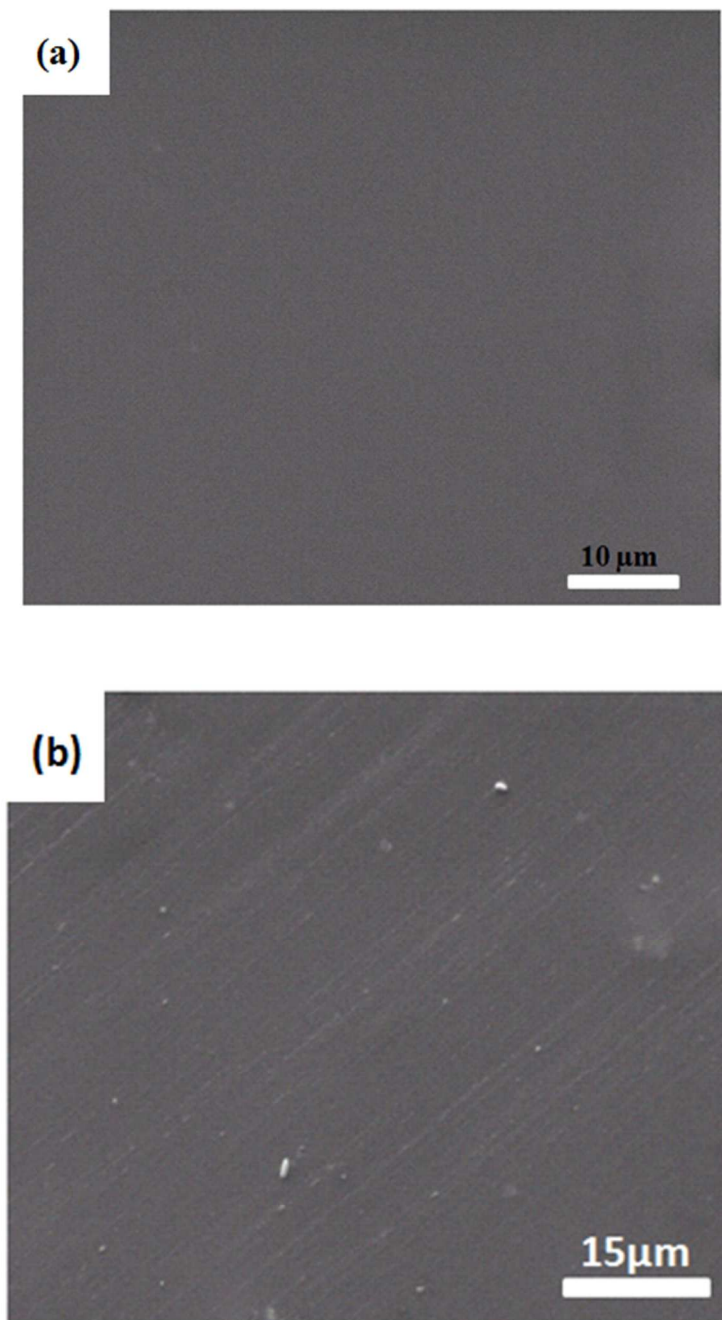


Figure 2

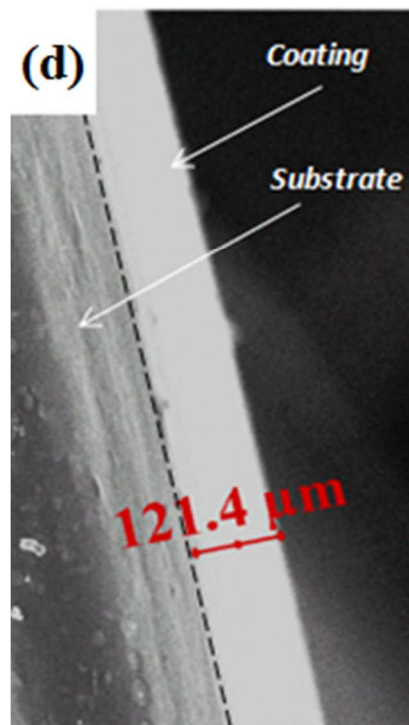
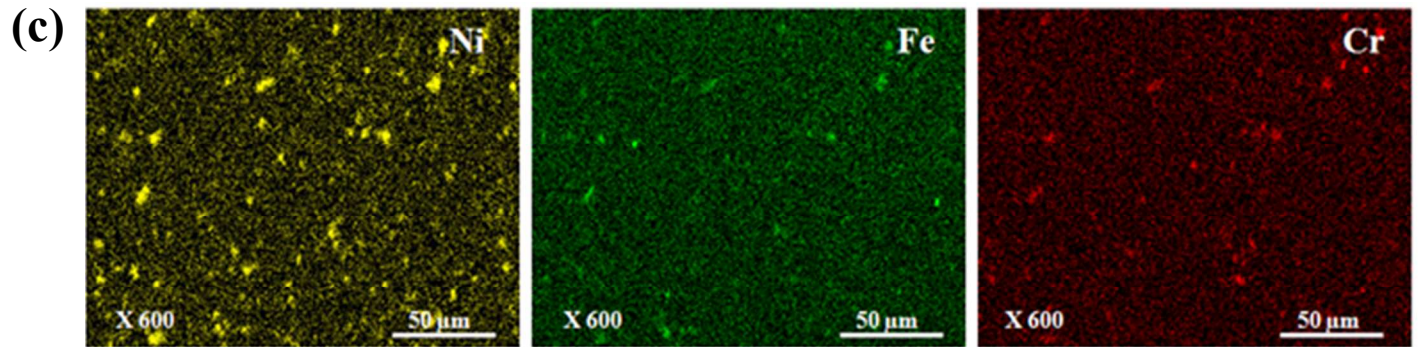
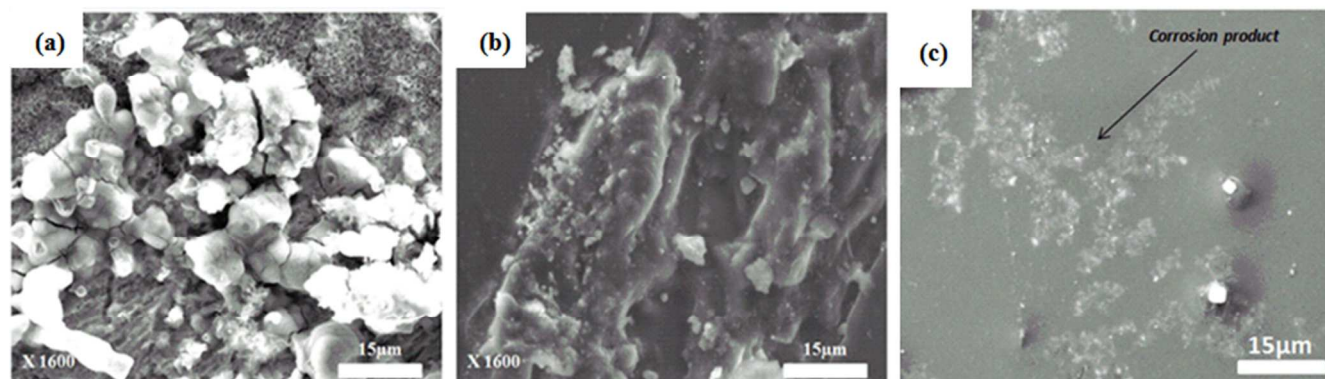


Figure 2



**Figure 3**

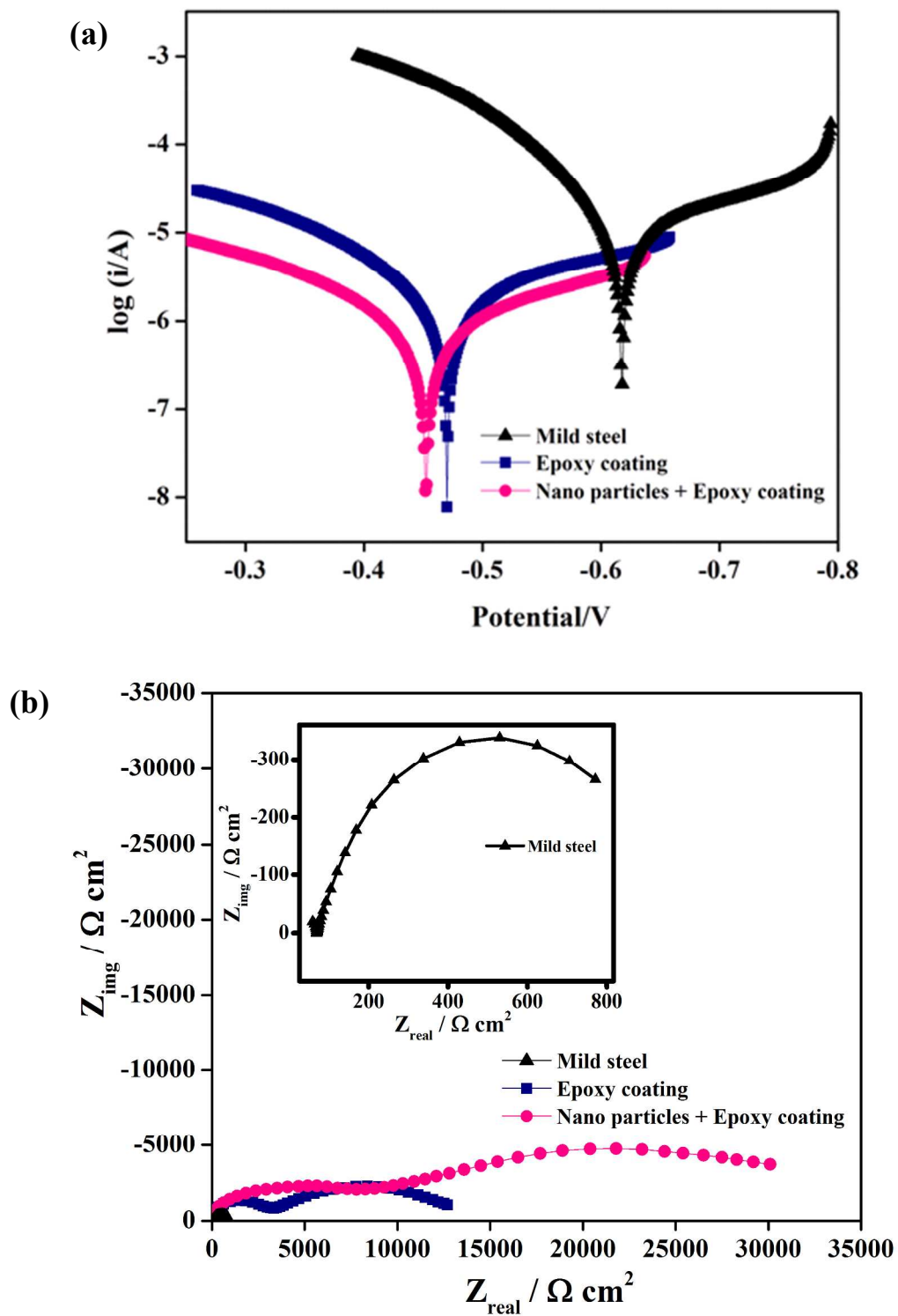


Figure 4

(C)

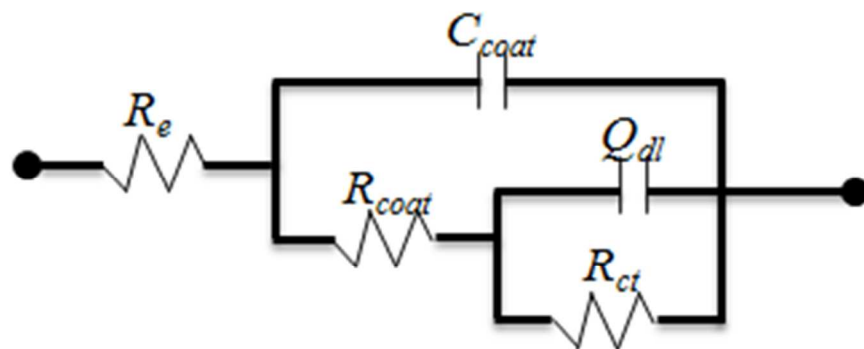


Figure 4